Journal Name

ARTICLE

Singlet excitation in the intermediate magnetic equivalence regime and field-dependent study of singlet-triplet leakage

Received 00th January 20xx,
Accepted 00th January 20xx

DOI: 10.1039/x0xx00000x

www.rsc.org/

Boris Kharkov, [a] Xueyou Duan, [b] Emily S. Tovar, [b] James W. Canary [b] and Alexej Jerschow *[b]

The examination and optimized preparation of nuclear spin singlet order has enabled the development of new types of applications that rely on potentially long-term polarization storage. Lifetimes several orders of magnitude longer than T_1 have been observed. The efficient creation of such states relies on special pulse sequences. The extreme cases of very large and very small magnetic equivalence received main attention, while relatively little effort has been directed towards studying singlet relaxation in intermediate regime. The intermediate case is of interest as it is relevant for many spin systems, and would also apply to heteronuclear systems in very low magnetic fields. Experimental evidence for singlet-triplet leakage in the intermediate regime is sparse. Here we describe a pulse sequence for efficiently creating singlets in the intermediate regime in a broad-band fashion. Singlet lifetimes are studied with a specially synthesized molecule over a wide range of magnetic fields using a home-built sample-lift apparatus. The experimental results are supplemented with spin simulations using parameters obtained from ab initio calculations. This work indicates that the chemical shift anisotropy (CSA) mechanism is relatively weak compared to singlet-triplet leakage for the proton system observed over a large magnetic field range. These experiments provide a mechanism for expanding the scope of singlet NMR to a larger class of molecules, and provide new insights into singlet lifetime limiting factors.

Introduction

A pair of nuclear spins-1/2 can form a singlet state, which can be protected from the environment under certain conditions.[1, 2] As a result, such states can exhibit lifetimes often significantly longer than those set by spin-lattice relaxation.[3-10] Life-times as long as 26 mins and 1 hr were reported for ^{15}N and ^{13}C singlets, respectively.[2, 11] Due to their extended life-times, singlet states have enabled new types of measurements, such as imaging of slow dynamic processes,[12, 13] the study of slow transport processes,[14-16] the measurement of molecular parameters,[17, 18] and the study of protein folding.[19] Notably, in the context of hyperpolarization and sensitivity enhancement, singlet states have been examined for their ability to store polarization over extended times.[20, 21]

The nature of singlet lifetime limiting factors has been the subject of intense research,[22, 23] in the course of which weak relaxation mechanisms, such as the spin-internal motion (related to spin-rotation), have come to light.[2, 6] A full understanding of these mechanisms, as well as the ability to reliably predict singlet lifetimes is currently lacking.

Methods for access to nuclear spin singlet states for initiation and readout can vary in their difficulty. For example, when the two spins are perfectly symmetric with respect to their coherent interactions (Zeeman and scalar coupling interactions[24, 25]), then the singlet state cannot be directly accessed by radio frequency (rf) irradiation alone.[26] In such cases, one can initiate the state, for example with a reaction, such as para-hydrogen addition, and one may read out the state via a chemical desymmetrization reaction.[23]

For non-negligible chemical or magnetic inequivalence between the two spins, generally two regimes have received attention. (1) Strong inequivalence: in this case, the differences in the coherent interactions are large enough, so that singlet-triplet conversion is rapid, and relatively simple pulse sequences can be employed to perform the conversion.[3, 15, 26-28] (2) Weak inequivalence: in this case, the coherent interactions by themselves are not sufficiently strong to provide an efficient transfer, and they can be modulated by special pulse sequences. Spin-Lock Induced Crossing (SLIC)[21, 23, 29-31] and *J*-coupling synchronized 180° pulse trains (M2S)[32-34] are the two most widely used experimental methods for this regime. Both work on the basis of satisfying a resonance condition that brings singlet and triplet states into contact. Another option for weak inequivalence is the use of static and rf field sweeps.[35, 36]

The intermediate regime is difficult to address with these methods. For example, the inequivalence may be just too small, so that spontaneous singlet-triplet oscillations are not efficient enough, and it may be too strong, so that a scheme, such as M2S would reduce to 1 or 2 inefficient cycles. General

[a] *Laboratory of Biomolecular NMR, Saint Petersburg State University, Saint Petersburg, Russia.*
[b] *Department of Chemistry, New York Unviersity, New York, NY 10003.*
* corresponding author: alexej.jerschow@nyu.edu.
Electronic Supplementary Information (ESI) available: [details of any supplementary information available should be included here]. See DOI: 10.1039/x0xx00000x

approaches, such as the adiabatic-passage spin order conversion[37, 38] or optimal control optimized pulses,[39, 40] perform very well regardless of the magnetic equivalence regime in the system. Their limitations, however, are that they are not broadband and are sensitive to B_0 inhomogeneity. For optimized pulse waveforms, another practical limitation is that it requires recalculating the pulse shape for every spin-system or change of conditions. A chemical shift scaling (CSS) approach has been used previously to achieve conditions of level anticrossings for singlet-triplet transitions, but requires the availability of additional spin groups.{Graafen, 2016 #39}

Relatively little is known about the influence of the singlet-triplet leakage on singlet lifetimes in the intermediate case.

In this work, we provide methodology for efficient and broad-band singlet-triplet conversion in the intermediate regime. This is achieved by combining CSS with M2S/S2M conversion. In addition, this technique is used to determine the behaviour of the singlet-triplet relaxation mechanism in a field-dependent study. A specifically synthesized test molecule displaying an intermediate chemical inequivalence case for protons is used. By employing a specially designed sample lift apparatus, the singlet lifetimes are observed over inequivalence regimes ranging from weak to intermediate. The experimental work is supplemented by spin simulations and ab initio calculations of chemical shift anisotropy (CSA) parameters combined with a conformational search. It is found that singlet-triplet leakage is the biggest field-dependent contributor to relaxation over the whole range, and that chemical shift anisotropy provides a relatively weak effect.

Materials and Methods

Compound synthesis. The half ester **1** was synthesized by a modified procedure from Ref. 1 and used directly for the next step without purification. To a suspension of maleic anhydride (420 mg, 4.28 mmol) in CH_2Cl_2 (8 mL) were added 2-propanol-d_8 (328 mg, 4.28 mmol) followed by Et_3N (0.65 mL, 4.66 mmol). The reaction mixture was heated under reflux for 15 min. After cooling to room temperature, the reaction was quenched with 2M HCl (10 mL) and the layers were separated and the organic phase was collected. The aqueous layer was saturated with NaCl and extracted three times with CH_2Cl_2. The combined organic layers were dried with anhydrous Na_2SO_4 and concentrated under vacuum, affording half ester **1** (706.6 mg, 95%) as a colorless oil. ^{1}H NMR (600 MHz, $CDCl_3$) δ 8.72 (br, ^{1}H), 6.39 (d, J = 12 Hz, ^{1}H), 6.33 (d, J = 12 Hz, ^{1}H). ^{13}C NMR (100 MHz, $CDCl_3$) δ 166.78, 166.43, 133.51, 131.10. MS (EI) calc. for $C_7H_3D_7O_4$ 165.2, found 166.2. To synthesize 1-(iso-propyl-d_7) 4-(tert-butyl-d_9) (Z)-but-2-enedioate **2**, concentrated sulfuric acid (0.069 mL, 1.25 mmol) was added to a suspension of anhydrous magnesium sulfate (0.60 g, 5 mmol) in 5 mL of dichloromethane while vigorously stirring. The mixture was stirred for 15 min, after which compound **1** (226 mg, 1.25 mmol) was added, followed by *tert*-butanol-d_{10} (0.114 mL, 1.5 mmol). The mixture was stirred at room temperature for 18h. The reaction mixture was then quenched with 20 mL of saturated sodium bicarbonate solution. The organic phase was collected and then washed with brine, dried with anhydrous sodium sulfate and finally concentrated. The asymmetric ester **2** was obtained (208 mg, 82%) after column chromatography. ^{1}H NMR (400 MHz, $CDCl_3$) δ 6.03 (q, 2H). ^{13}C NMR (100 MHz, $CDCl_3$) δ 165.02, 164.57, 131.29, 128.99. ^{2}H NMR (61.4 MHz, $CDCl_3$) δ 5.01 (s, 1D), 1.38 (s, 9D), 1.16 (s, 6D).

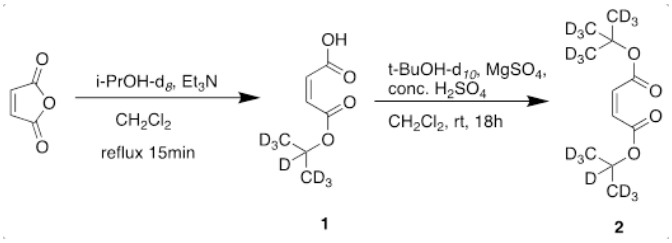

Scheme 1 Molecular structure and synthesis of deuterated *tert*-butyl propyl maleate diester **2**.

NMR sample preparation. A sample of 5 mM solution of the ester **2** in deuterated chloroform was degassed in a 5 mm NMR tube using a Schlenk line. Five consecutive cycles of degassing under vacuum were applied. In each cycle, the sample was frozen with liquid nitrogen, kept under vacuum for three minutes and then thawed. To assess the quality of degassing, the T_1 of residual ^{1}H nuclei in deuterated chloroform was measured to be 322 s, which indicated a good performance of the degassing procedure. To avoid convection effects,[34] the height of the solution in the NMR tube was limited to 6 mm and the sample was placed well within the coil volume.

NMR experiment. Singlet and T_1 relaxation experiments were performed using a Bruker AV-500 (500 MHz) spectrometer equipped with a standard solution-state triple resonance BBO probe. The experiments were performed at ambient temperature (293 K). The longitudinal relaxation time (T_1) was measured using the standard saturation recovery technique. The radio frequency field strength in T_1 and M2S/CSS (CSS stands for chemical shift scaling) experiments was $\gamma B_1/2\pi = 13.9\ \mathrm{kHz}$. The M2S/CSS pulse sequence parameters were set up based on the vinylene proton-proton J-coupling and the in-singlet chemical shift difference measured from a 1D proton spectrum (details in the ESI). The measured values were $J = 12\ \mathrm{Hz}$ and $\Delta\delta = 2.4 \times 10^{-2}\ \mathrm{ppm}$ (12 Hz at B_0 = 500 MHz). Composite pulses (90°-180°-90°) were used for refocusing in the M2S J-synchronized blocks, cycled according to the MLEV-4 scheme (x, x, -x, -x). To reduce heating of the sample, non-composite 180° pulses were used for refocusing in the CSS pulse trains. The number of pulses per one CSS block was 8, although any multiple of 8 can be used to meet the phase cycle requirements. The phases of the pulses followed an XY-8 cycle (x, y, x, y, y, x, y, x).[41] The echo delay in the M2S pulse sequence was optimized to $\tau_J/4 = 21.1\ \mathrm{ms}$. The chemical shift scaling factor was chosen to be equal to 10 (see description of the pulse sequence below) so that the characteristic delays were $\tau_1 = 18.99\ \mathrm{ms}$ and $\tau_2 = 2.11\ \mathrm{ms}$ (see Figure 1 and Equation 5). The echo numbers in M2S were optimized to $n_1 = 12$ and $n_2 = 6$. These values were lower than expected for the

scaled chemical shift (16 and 8, respectively). This discrepancy indicated that the effective chemical shift difference was somewhat higher than the anticipated value of 2.4×10^{-3} ppm (chemical shift difference after downscaling with a CSS factor of 10), indicating suboptimal performance of the chemical shift scaling part of the pulse sequence. Additionally, it was noted that there was no reduction of the effective chemical shift when the CSS scaling factor was further increased, which could be attributed to imperfections in the CSS pulse train.

Field cycling. A home-built automated pulse-sequence-synchronized sample lift was used (see description in the ESI). This lift allows moving the sample to different magnetic field regions in the range from 0.06 T to 11.74 T. The time needed for the device to lift and lower the sample did not exceed 2.2 sec for the sample rise distance of 65 cm. The lowering and raising times, as well as any intermediate relaxation effects can be considered constant for a given set of experiments.

Ab initio calculations Optimized geometries and CSA tensors were calculated using Gaussian16. Conformations were generated in OpenBabel using the Confab algorithm (10,000 conformations with 10 kcal/mol energy cutoff resulted in 12 output conformations). Geometry optimization was performed with an APFD functional and successive refinements were performed with the basis sets 6-31+G(d), 6-311G(d), 6-311+G(d), and 6-311+G(d, p). Convergence was tested with a frequency calculation, which led to 4 remaining unique and fully converged conformations. The distance between the nuclei in the vinyl group was determined to be 2.43 Å after conformational averaging. The tensors were subsequently obtained from a GIAO calculation with the 'spinspin' and 'mixed' keywords and an APFD/aug-cc-pVTZ combination. An ultra-fine grid was used throughout. Tensor values were subsequently conformationally averaged. The average norms of the differences between the CSA tensors of the two vinylene protons were 4.51 and 0.61 ppm for the symmetric and antisymmetric tensor components, respectively.

Numerical simulations were performed using the Spinach 2.1 package.[42] The CSA tensors obtained in the ab initio calculations were used. The in-singlet *J*-coupling value and the chemical shift difference were set to 12 Hz and 0.024 ppm, respectively. These values were obtained from the analysis of the 1D proton spectrum (see ESI).

Theory

The Hamiltonian of a two-spin-1/2 system in solution can be written as

$$H = 2\pi J\, \boldsymbol{I}\cdot\boldsymbol{S} + \frac{\omega_\Sigma}{2}(I_z + S_z) + \frac{\omega_\Delta}{2}(I_z - S_z), \qquad (1)$$

where $\omega_\Sigma = (\omega_I + \omega_S)$ and $\omega_\Delta = (\omega_I - \omega_S)$. The first term corresponds to the *J*-coupling interaction, and the Zeeman interaction is separated into symmetric and antisymmetric parts with respect to spin exchange. The second term disappears when transitioning to a corresponding rotating frame and will hence be omitted from further discussion. The symmetry properties of the system define the eigenstates of the Hamiltonian. For a weakly-coupled spin system ($\omega_\Delta \gg 2\pi J$), the eigenstates of the Hamiltonian are the Zeeman eigenstates $\{|\alpha\alpha\rangle, |\alpha\beta\rangle, |\beta\alpha\rangle, |\beta\beta\rangle\}$, while in case of strong coupling ($\omega_\Delta \ll 2\pi J$) the singlet and three triplet states would form the eigenbase, $\{|S_0\rangle, |T_{+1}\rangle, |T_0\rangle, |T_{-1}\rangle\}$. These two sets of states are related according to

$$|S_0\rangle = \frac{|\alpha\beta\rangle - |\beta\alpha\rangle}{\sqrt{2}}, \qquad (2a)$$

$$|T_{+1}\rangle = |\alpha\alpha\rangle, \qquad (2b)$$

$$|T_0\rangle = \frac{|\alpha\beta\rangle + |\beta\alpha\rangle}{\sqrt{2}}, \text{ and} \qquad (2c)$$

$$|T_{-1}\rangle = |\beta\beta\rangle. \qquad (2d)$$

The triplet states are symmetric with respect to spin index exchange, while the singlet state is antisymmetric. For this reason, in order to populate a singlet state, a symmetry breaking interaction, such as chemical shift difference or *J*-coupling imbalance, is required. The exact eigenstates, which are also valid in the intermediate regime, where the chemical shift difference is comparable to the *J*-coupling, are[4]

$$|S_0'\rangle = |S_0\rangle\cos\frac{\theta}{2} + |T_0\rangle\sin\frac{\theta}{2}, \qquad (3a)$$

$$|T_{+1}'\rangle = |T_{+1}\rangle, \qquad (3b)$$

$$|T_0'\rangle = |T_0\rangle\cos\frac{\theta}{2} - |S_0\rangle\sin\frac{\theta}{2}, \qquad (3c)$$

$$|T_{-1}'\rangle = |T_{-1}\rangle, \qquad (3d)$$

where the singlet-triplet mixing angle is given by

$$\theta = \arctan\left(\frac{\omega_\Delta}{2\pi J}\right). \qquad (4)$$

If this angle is large, it is straightforward to convert triplet states to singlet state, because evolution under the Hamiltonian would perform the necessary symmetry-breaking operation. Specific pulse sequences can be used for this purpose.[3, 15, 26-28] Typically, for such experiments, also a strong spin-lock or decoupling sequence would be required to preserve the singlet state.[7]

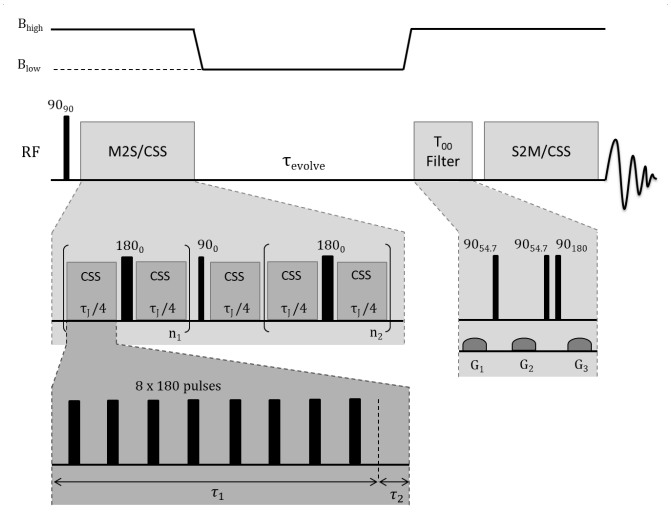

Figure 1 An M2S/CSS experimental technique. The CSS pulse sequence is introduced in the *J*-synchronized delays of the M2S and S2M singlet preparation and detection blocks.

At the opposite end of the spectrum, if θ is small, spontaneous singlet-triplet conversion cannot be achieved. It is, however, possible to modulate the antisymmetric Zeeman term by the application of either a weak spin-lock (SLIC),[29] or a sequence of properly spaced 180° pulses (M2S).[33] If this modulation frequency matches the *J*-coupling constant, an efficient transition between triplet and singlet states can be achieved.

Between those two regimes, however, it is not clear how an efficient transfer could be performed. For example, free evolution would not provide sufficient symmetry breaking, and the M2S sequence is ineffective. In particular, n_1 and n_2 become too small and cannot be adjusted properly. The M2S pulse sequence scheme demonstrates its optimal performance when ω_Δ is much smaller than the *J*-coupling. In this case, the numbers of *J*-synchronized echo blocks, n_1 and n_2, are large and can be tuned to match the optimal transfer conditions. To bring the intermediate regime into the region of effectiveness of the M2S sequence, the asymmetric part of the Hamiltonian is reduced using a CSS sequence.[43] In the CSS sequence, a train of 180°-pulses refocuses the chemical shift interaction during the period τ_1 and keeps it unperturbed only during the short period of time τ_2. The effective amplitude of the antisymmetric Zeeman Hamiltonian then becomes[43]

$$\tilde{\omega}_\Delta = \frac{\tau_2}{\tau_1+\tau_2}\omega_\Delta. \qquad (5)$$

The optimal triplet-to-singlet transfer conditions in this case are $n_1\tilde{\theta} \approx \pi$, $2n_2\tilde{\theta} \approx \pi$, where

$$\tilde{\theta} = \arctan\left(\frac{\tilde{\omega}_\Delta}{2\pi J}\right). \qquad (6)$$

The CSS blocks modify the effective Hamiltonian but do not influence the pathways of singlet/triplet transfer of the unmodified M2S pulse sequence. For this reason, the overall transfer efficiency of the pulse sequence does not change.

After generation of the singlet, the sample is transported to different magnetic field positions by the sample lift and stored in a lower field during the τ_{evolve}. The sample is put back to high field at the end of the τ_{evolve} delay.

During the period τ_{evolve}, the full unperturbed spin Hamiltonian acts on the created singlet population. The M2S sequence is designed to produce the $|S_0\rangle\langle S_0|$ state. Since $|S_0\rangle$ is not an eigenstate of the Hamiltonian, and can be written as (see Eq. (3a))

$$|S_0\rangle = |S_0'\rangle \sec\frac{\theta}{2} + |T_0\rangle \tan\frac{\theta}{2}, \qquad (7)$$

parts of the created state will evolve coherently via the singlet-triplet coherences, $|S_0'\rangle\langle T_0'|$, and $|T_0'\rangle\langle S_0'|$. Since the components involving $|T_0'\rangle$ typically relax faster than $|S_0'\rangle$, after some period of time, the spin system can be described by the tilted state $|S_0'\rangle\langle S_0'|$ alone. In the following, we refer to $|S_0'\rangle\langle S_0'|$ relaxation as singlet relaxation. After the relaxation interval, the $|S_0\rangle\langle S_0|$ projection is converted back to the transverse magnetization by the S2M part of the sequence, which also contains the CSS elements in the intervals of the *J*-synchronization.

The singlet-triplet precession during the relaxation delay τ_{evolve} leads to additional oscillations in the relaxation curve. To avoid such spin dynamics, two experimental strategies can be used. One can simply wait until these components decay, which may lead to additional losses in sensitivity. The approach used in this work, is to average over the oscillations. To do so, for each time point *t* on the relaxation curve, a number *k* of data points, equally spaced in time {*t*, *t+T*, *t+2T*, …, *t+(k-1)T*} are measured. The time spacing interval *T* between data acquisitions is k times smaller than the precession period and equals to

$$T = \frac{2\pi}{\omega_{\text{eff}}\, k}, \qquad (8)$$

$$\omega_{\text{eff}} = \sqrt{{\omega_\Delta}^2 + (2\pi J)^2}\,. \qquad (9)$$

Using this averaging scheme, the influence of the evolution of the part of the spin state that does not commute with the Hamiltonian can thus be minimized even at short relaxation delays.

Results and discussion

We applied the M2S/CSS experimental technique to study the field dependence of singlet relaxation in compound **2**. The chemical shift difference was 0.024 ppm and the in-pair coupling was 12 Hz, making the angle θ = 45° at a field of 11.74 T. In this regime, intermediate magnetic (and chemical) inequivalence was found for the vinylene protons. To study the effect of singlet-triplet leakage on the singlet lifetime, we varied the field B_0, and thus the singlet-triplet mixing angle θ (Eq. 4), during the relaxation delay over the range from 0.03 to 11 T. To achieve this, the sample tube was transferred from the magnet coil to a predetermined position in the magnet bore with the desired field strength (see details in ESI). Figure 2 shows the $|S_0\rangle\langle S_0|$ projection of the spin state during its time evolution under the effect of the local field described by the Hamiltonian in Eq. (1). The frequency of the observed singlet-triplet coherence oscillations was 17.1 Hz at 11.74 T, which was in good agreement with the expected value of 17 Hz based on the measured *J*-coupling and chemical shift difference values (12 Hz and 0.024 ppm, respectively), according to Eq. (9). The observed oscillations make it necessary to use an averaging procedure as described for accurately sampling the points for small τ_{evolve} values, as described in the theory section. In the present set of measurements, the number of averaging steps *k* was 4. An example of the singlet relaxation decay obtained using the averaging procedure at $B_{low} = 11$ *T* is presented in Figure 2b. As can be seen, the undesired spin dynamics is avoided by this procedure and a clean singlet-relaxation decay can be observed.

Figure 3 shows the field dependence of the obtained $|S_0'\rangle\langle S_0'|$ relaxation rates. The results of a numerical simulation

of the relaxation are shown by the solid line. The dashed line indicates the simulated relaxation field dependence without CSA relaxation taken into account. The correlation time obtained from the fitting was 21 ps which was lower than the 30 ps estimated from the T_1 = 10 s for the vinyl protons. This discrepancy could be explained by the fact that the *ab initio* CSA tensor calculation produced somewhat higher average values, and/or that conformational averaging led to a further reduction of the relaxation effects.

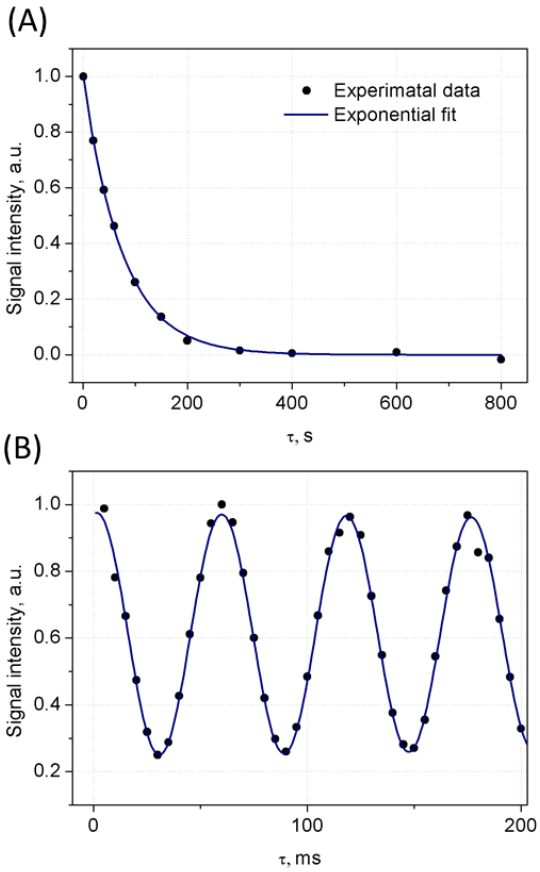

Figure 2 (A) Singlet relaxation decay obtained after averaging signal precession at the field B_{low} = 11 T. (B) Singlet-triplet oscillations due to precession around the tilted effective field (Eq. 1) at 11.74 T.

Two mechanisms that explicitly depend on the B_0 field strength are the CSA relaxation and singlet-triplet leakage (in a chemically inequivalent system). Both these relaxation mechanisms vanish at zero field. At low fields, one can see the contribution of other mechanisms, such as e.g. spin-rotation and spin-internal motion,[22] indirect dipole relaxation,[44] and out-of-pair inter- and intra-molecular dipole relaxation.[22] Of these, the dominant mechanism is most likely the spin-internal motion relaxation. The contribution from the direct out-of-pair dipole relaxation can be neglected by deuteration of the molecular side-chains and the solvent. These relatively field-independent contributions amount to a rate contribution of 1.95×10^{-3} s^{-1}. Scalar relaxation of the second kind[44] was considered as a contributing mechanism, but was thought to be unimportant in this case, because applying a spin-lock field at high field actually led to a shortening of the lifetime. A lengthening would be observed if this mechanism were prominent.[44] At fields above 3-4 T the singlet leakage becomes the dominant relaxation mechanism. The contribution of the CSA relaxation remains small compared to other relaxation mechanisms in the whole B_0 range. As can be seen in Figure 3, CSA produces a relatively minor contribution to singlet relaxation, with the largest portion arising from singlet-triplet leakage alone.

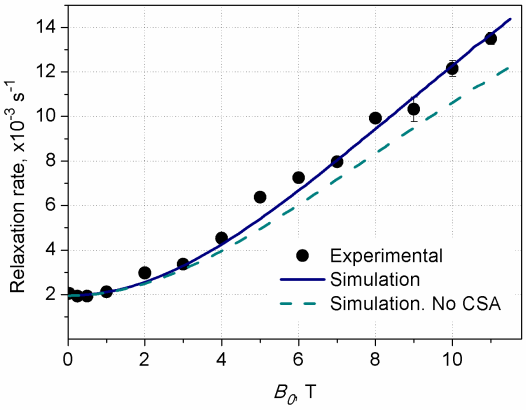

Figure 3 The field dependence of the singlet relaxation rate.

The presented results show that the developed technique affords a mechanism for studying singlet relaxation. Although one could design an optimal pulse waveform for singlet-to-triplet conversion in the intermediate case, its implementation can be impractical due to the low generality of application, since it is necessary to recalculate the pulse shape when the external field or the system under study changes. By contrast, the M2S-CSS scheme employed here provides a very clear procedure for tuning the sequence to the specific molecules under study. In a typical sequence setup procedure, one can first define the CSS scaling factor, based on estimates of the chemical shift difference in the system, and set the delays τ_1 and τ_2 as fractions of the *J*-synchronization delay $\tau_J/4$. After that, parameters $\tau_J/4$, n_1, and n_2 are adjusted as it is typically performed for the M2S sequence, by searching for the maximum signal detected in the end of the pulse sequence. As the CSS scaling factor and repetition numbers n_1, and n_2 are interdependent, one can be adjusted while the other is fixed and *vice versa*.

Conclusions

In this article, we presented a new experimental technique for singlet relaxation measurements in the intermediate magnetic equivalence regime ($\omega_\Delta \sim 2\pi J$). The pulse sequence relies on a chemical shift scaling sequence combined with the M2S conversion scheme, which produces robust and broadband triplet-singlet-triplet conversion. The pulse sequence is flexible and can be used in a wide range of external fields. Using the presented method, in combination with a home-built field-

cycling setup, the relative contributions of singlet relaxation were studied over a large magnetic field range. The obtained results show that relaxation appears to be caused by a minor constant relaxation contribution in combination with primarily singlet-triplet leakage, followed by a relatively weak CSA contribution. The experimental results are well represented by simulations using geometries and CSA tensors obtained from *ab initio* calculations.

Conflicts of interest

There are no conflicts to declare with regard to the subject matter.

Acknowledgements

This work was supported by NSF grants CHE-1412568 and grant CHE-1710046, as well as a Diamond Jubilee Visiting Fellowship. E.S.T. was supported by an NSF REU grant (REU in Chemical Biology at NYU). The experiments were performed in the Shared Instrument Facility of the Department of Chemistry, New York University, supported by the US National Science Foundation under Grant No. CHE0116222. The Bruker Avance-500 NMR Spectrometer was acquired through the support of the National Science Foundation under Award Number CHE-01162222. We acknowledge stimulating and enlightening discussions with Malcolm H. Levitt.

References

1. M. Carravetta, O. G. Johannessen and M. H. Levitt, *Phys. Rev. Lett.*, 2004, **92**, 153003.
2. G. Stevanato, J. T. Hill-Cousins, P. Håkansson, S. S. Roy, L. J. Brown, R. C. D. Brown, G. Pileio and M. H. Levitt, *Angew. Chem. Int. Ed.*, 2015, **54**, 3740.
3. M. Carravetta and M. H. Levitt, *J. Am. Chem. Soc.*, 2004, **126**, 6228.
4. M. Carravetta and M. H. Levitt, *J. Chem. Phys.*, 2005, **122,** 214505.
5. A. K. Grant and E. Vinogradov, *J. Magn. Reson.*, 2008, **193**, 177.
6. G. Pileio, J. T. Hill-Cousins, S. Mitchell, I. Kuprov, L. J. Brown, R. C. D. Brown and M. H. Levitt, *J. Am. Chem. Soc.*, 2012, **134**, 17494.
7. G. Pileio and M. H. Levitt, *J. Chem. Phys.*, 2009, **130**, 214501.
8. E. Vinogradov and A. K. Grant, *J. Magn. Reson.*, 2007, **188**, 176.
9. W. S. Warren, E. Jenista, R. T. Branca and X. Chen, *Science*, 2009, **323**, 1711.
10. M. Carravetta, O. G. Johannessen and M. H. Levitt, *Phys. Rev. Lett.*, 2004, **92**, 153003.
11. G. Pileio, M. Carravetta, E. Hughes and M. H. Levitt, *J. Am. Chem. Soc.*, 2008, **130**, 12582.
12. J. N. Dumez, J. T. Hill-Cousins, R. C. D. Brown and G. Pileio, *J. Magn. Reson.*, 2014, **246**, 27.
13. G. Pileio, J. N. Dumez, I. A. Pop, J. T. Hill-Cousins and R. C. D. Brown, *J. Magn. Reson.*, 2015, **252**, 130.
14. S. Cavadini, J. Dittmer, S. Antonijevic and G. Bodenhausen, *J. Am. Chem. Soc.*, 2005, **127**, 15744.
15. R. Sarkar, P. R. Vasos and G. Bodenhausen, *J. Am. Chem. Soc.*, 2007, **129**, 328.
16. P. Ahuja, R. Sarkar, P. R. Vasos and G. Bodenhausen, *J. Am. Chem. Soc.*, 2009, **131**, 7498.
17. P. Ahuja, R. Sarkar, P. R. Vasos and G. Bodenhausen, *J. Chem. Phys.*, 2007, **127**, 134112.
18. M. C. D. Tayler, S. Marie, A. Ganesan and M. H. Levitt, *J. Am. Chem. Soc.*, 2010, **132**, 8225.
19. N. Salvi, R. Buratto, A. Bornet, S. Ulzega, I. Rentero Rebollo, A. Angelini, C. Heinis and G. Bodenhausen, *J. Am. Chem. Soc.*, 2012, **134**, 11076.
20. P. R. Vasos, A. Comment, R. Sarkar, P. Ahuja, S. Jannin, J.-P. Ansermet, J. A. Konter, P. Hautle, B. van den Brandt and G. Bodenhausen, *Proc. Natl. Acad. Sci. U.S.A.*, 2009, **106**, 18469.
21. Y. Zhang, K. Basu, J. W. Canary and A. Jerschow, *Phys. Chem. Chem. Phys.*, 2015, **17**, 24370.
22. G. Pileio, *Prog. Nucl. Mag. Res. Sp.*, 2010, **56**, 217.
23. Y. Zhang, X. Duan, P. C. Soon, V. Sychrovský, J. W. Canary and A. Jerschow, *ChemPhysChem*, 2016, **17**, 2967.
24. M. B. Franzoni, L. Buljubasich, H. W. Spiess and K. Munnemann, *J. Am. Chem. Soc.*, 2012, **134**, 10393.
25. Y. Feng, T. Theis, X. Liang, Q. Wang, P. Zhou and W. S. Warren, *J. Am. Chem. Soc.*, 2013, **135**, 9632.
26. M. H. Levitt, *Annu. Rev. Phys. Chem.*, 2012, **63**, 89.
27. D. Graafen, M. B. Franzoni, L. M. Schreiber, H. W. Spiess and K. Munnemann, *J. Magn. Reson.*, 2016, **262**, 68.
28. G. Stevanato, S. S. Roy, J. Hill-Cousins, I. Kuprov, L. J. Brown, R. C. D. Brown, G. Pileio and M. H. Levitt, *Phys. Chem. Chem. Phys.*, 2015, **17**, 5913.
29. S. J. DeVience, R. L. Walsworth and M. S. Rosen, *Phys. Rev. Lett.*, 2013, **111**, 173002.
30. Y. Feng, T. Theis, T. L. Wu, K. Claytor and W. S. Warren, *J. Chem. Phys.*, 2014, **141**, 134307.
31. T. Theis, Y. Feng, T. Wu and W. S. Warren, *J. Chem. Phys.*, 2014, **140**, 014201.
32. G. Pileio, M. Carravetta and M. H. Levitt, *Proc. Natl. Acad. Sci. U.S.A.*, 2010, **107**, 17135.
33. M. C. D. Tayler and M. H. Levitt, *Phys. Chem. Chem. Phys.*, 2011, **13**, 5556.
34. B. Kharkov, X. Duan, J. W. Canary and A. Jerschow, *J. Magn. Reson.*, 2017, **284**, 1.
35. L. Buljubasich, M. B. Franzoni, H. W. Spiess and K. Munnemann, *J. Magn. Reson.*, 2012, **219**, 33.
36. M. B. Franzoni, D. Graafen, L. Buljubasich, L. M. Schreiber, H. W. Spiess and K. Munnemann, *Phys. Chem. Chem. Phys.*, 2013, **15**, 17233.
37. A. N. Pravdivtsev, A. S. Kiryutin, A. V. Yurkovskaya, H. M. Vieth and K. L. Ivanov, *J. Magn. Reson.*, 2016, **273**, 56.
38. A. S. Kiryutin, A. N. Pravdivtsev, A. V. Yurkovskaya, H. M. Vieth and K. L. Ivanov, *J. Phys. Chem. B*, 2016, **120**, 11978.
39. C. Laustsen, S. Bowen, M. S. Vinding, N. C. Nielsen and J. H. Ardenkjaer-Larsen, *Magnetic Resonance in Medicine*, 2014, **71**, 921-926.
40. B. A. Rodin, A. S. Kiryutin, A. V. Yurkovskaya, K. L. Ivanov, S. Yamamoto, K. Sato and T. Takui, *J. Magn. Reson.*, 2018, **291**, 14.
41. T. Gullion, D. B. Baker and M. S. Conradi, *J. Magn. Reson. (1969)*, 1990, **89**, 479.

42. H. J. Hogben, M. Krzystyniak, G. T. P. Charnock, P. J. Hore and I. Kuprov, *J. Magn. Reson.*, 2011, **208**, 179.
43. G. A. Morris, N. P. Jerome and L. Y. Lian, *Angew. Chem. Int. Ed. Engl.*, 2003, **42**, 823.
44. G. Pileio, *J. Chem. Phys.*, 2011, **135**, 174502.